Kobe University Repository : Kernel

PDF issue: 2026-11-15

Structural Determinants of the Position of 2,3',4,4',5-Pentachlorobiphenyl (CB118) Hydroxylation by Mammalian Cytochrome P450 Monooxygenases

Mise, Shintaro ; Haga, Yuki ; Itoh, Toshimasa ; Kato, Akira ; Fukuda, Itsuko ; Goto, Erika ; Yamamoto, Keiko ; Yabu, Miku ; Matsumura,…

(Citation)
Toxicological Sciences,152(2):340-348

(Issue Date)
2016-08

(Resource Type)
journal article

(Version)
Accepted Manuscript

(Rights)
©The Author 2016. Published by Oxford University Press on behalf of the Society of Toxicology. This is a pre-copyedited, author-produced version of an article accepted for publication in [Toxicological Sciences] following peer review. The version of record [Toxicological Sciences. 152(2): 340-348, Aug 2016] is available online at:…

(URL)
https://hdl.handle.net/20.500.14094/90003690

Structural determinants of the position of 2,3′,4,4′,5-pentachlorobiphenyl (CB118) hydroxylation by mammalian cytochrome P450 monooxygenases

Shintaro Mise*, Yuki Haga†, Toshimasa Itoh‡, Akira Kato‡, Itsuko Fukuda*,§,¶, Erika Goto¶, Keiko Yamamoto‡, Miku Yabu*, Chisato Matsumura†, Takeshi Nakano||, Toshiyuki Sakaki|||, and Hideyuki Inui*,¶,||||

*Graduate School of Agricultural Science, Kobe University, Kobe, Hyogo 657-8501, Japan; †Hyogo Prefectural Institute of Environmental Sciences, Kobe, Hyogo 654-0037, Japan; ‡Laboratory of Drug Design and Medicinal Chemistry, Showa Pharmaceutical University, Machida, Tokyo 194-8543, Japan; §Research Center for Food Safety and Security, Kobe University, Kobe, Hyogo 657-8501, Japan; ¶Faculty of Agriculture, Kobe University, Kobe, Hyogo 657-8501, Japan; ||Research Center for Environmental Preservation, Osaka University, Suita, Osaka 565-0871, Japan; |||Biotechnology Research Center, Faculty of Engineering, Toyama Prefectural University, Imizu, Toyama 939-0398, Japan; and ||||Research Center for Environmental Genomics, Kobe University, Kobe, Hyogo 657-8501, Japan

Address correspondence to: Hideyuki Inui, Research Center for Environmental Genomics, Kobe University, 1-1 Rokkodai-cho, Nada-ku, Kobe, Hyogo 657-8501, Japan. Tel. & Fax:

+81-78-803-5863; E-mail: hinui@kobe-u.ac.jp

Running title: Structural basis of PCB hydroxylation by P450

ABSTRACT

Polychlorinated biphenyls (PCBs) accumulate in mammals via the food chain because of their characteristics such as slow degradation and high hydrophobicity. One of the 209 PCB congeners, 2,3',4,4',5-pentachlorobiphenyl (CB118), is abundantly found in the environment and in mammals. Understanding the metabolic fate of CB118 can provide important information toward evaluating its toxicity. *In vitro* studies on the metabolism of CB118 by cytochrome P450 enzymes (P450 or CYP) revealed that human CYP2B6 and rat CYP2B1 primarily metabolized it to 3-hydroxy (OH)-CB118, whereas rat CYP1A1 metabolized CB118 to 4-hydroxy-2,3,3',4',5-pentachlorobiphenyl (4-OH-CB107). Docking models of CYP2Bs with CB118 revealed a short distance between the 3-position of CB118 and the heme iron caused by polarization of the substrate-binding cavity, and maintenance of this pose through interaction with the peripheral amino acids determines the activity and position of hydroxylation. 4-Hydroxylation by rat CYP1A1 occurs owing to the longitudinal shape of the substrate-binding cavity toward the heme of CYP1A1. The metabolites 3-OH-CB118 and 4-OH-CB107 decreased potential for activating the aryl hydrocarbon receptor compared to that of CB118, thereby leading to a decrease in dioxin-like toxicity; however, the neurodevelopmental toxicity of 4-OH-CB107 has been previously reported. The results suggest that these three P450 isoforms play an important role in determining the extent of CB118 toxicity. This study will contribute to understanding of the metabolic fates and toxicity of CB118 *in vivo*.

Keywords: cytochrome P450 monooxygenase, docking model, hydroxylation, polychlorinated biphenyl, 3D structure

INTRODUCTION

Polychlorinated biphenyls (PCBs) are serious environmental and biological contaminants because of their low degradation properties, extremely high hydrophobicity, and capacity for long-distance migration. These characteristics are persistent in the environment, leading to high accumulation in apex species, including humans. Consequently, various diseases and disorders such as reproductive impairments, endocrine disruption, and metabolic disorders are developed. The World Health Organization has defined toxic equivalency factors (TEFs) for the toxicity levels of 12 PCBs relative to that of the most toxic compound 2,3,7,8-tetrachlorodibenzo-*p*-dioxin (TCDD) (Van den Berg *et al.*, 2006). Dioxin-like toxicity is caused by the activation of aryl hydrocarbon receptor (AhR), which is followed by its binding to the dioxin-responsive element (DRE) (Mimura and Fujii-Kuriyama, 2003). 2,3',4,4',5-Pentachlorobiphenyl (CB118), with a TEF value of 0.00003, is one of the most abundant congeners among the 209 PCBs in the environment including river sediments, algae, plants, shrimp, and fish (Nunes *et al.*, 2011) and in humans (Hirai *et al.*, 2005). Lake Baikal is a site that is highly contaminated by several anthropogenic sources, and Baikal seals contain high amounts of CB118 (Imaeda *et al.*, 2014). After ingestion of CB118, mainly through fish consumption, CB118 is metabolized to several hydroxylated metabolites, such as 4-hydroxy-2,3,3',4',5-pentachlorobiphenyl (4-OH-CB107) and 3-OH-CB118, which were found in human plasma (Quinete *et al.*, 2015) and in the liver of Baikal seals (Nomiyama *et al.*, 2014). In rats, 4-OH-CB107, 4-hydroxy-2,3',4',5-tetrachlorobiphenyl (4-OH-CB70), and 3-OH-CB118 accumulate in the blood

(Haraguchi *et al.*, 1998). In a previous report, we identified hydroxylated metabolites of 3,3',4,4',5-pentachlorobiphenol (CB126) generated by cytochrome P450 enzymes (P450 or CYP), especially by rat CYP1A1 (Yamazaki *et al.*, 2011). CYP1A is responsible for the metabolism of coplanar PCBs (Inui *et al.*, 2014). In contrast, the CYP2B subfamily is related to the metabolism of *ortho*-substituted PCBs such as 2,2',3,4',6-pentachlorobiphenyl (CB91) and 2,2',3,5',6-pentachlorobiphenyl (CB95) (Kania-Korwel *et al.*, 2011). Thus, hydroxylation of CB118 *in vivo* is performed by CYP1As and CYP2Bs. It was reported that human CYP2A6 showed a 4-hydroxylation activity toward 2,2',4',5,5'-pentachlorobiphenyl (McGraw and Waller, 2006). However, information on PCB metabolism by human P450 isoforms is limited.

Hydroxylation of xenobiotics leads to further detoxification followed by conjugation with glucuronic acid or sulfonate and finally excretion. However, it has been reported that 4-hydroxylated metabolites of PCBs disrupt homeostasis of thyroid hormone (Imaeda *et al.*, 2014) and Ca^{2+}, and membrane potential (Londoño *et al.*, 2009). For example, 4-OH-CB107, a major CB118 metabolite, decreased the level of plasma thyroid hormone, thyroxine (T_4), by competitively binding to the T_4 transport protein, transthyretin (Meerts *et al.*, 2004a; Meerts *et al.*, 2004b). Although hydroxylated metabolites of PCBs decrease toxicity through AhR activation, there is no information on the toxicity of 3-OH-CB118. These results suggest that hydroxylation of CB118 in mammals is critical for determining the extent of CB118 toxicity.

In this study, we elucidated the role of the P450 isoforms that metabolize CB118 in effecting toxicity

and analyzed the structural basis of CB118 hydroxylation. We conducted *in vitro* studies on CB118 metabolism using recombinant P450 isoforms to identify CB118 metabolites and employed docking models of the P450 isoforms with CB118 to propose critical determinants for selecting hydroxylation positions.

MATERIALS AND METHODS

Chemicals. CB118 and TCDD were purchased from AccuStandard (New Haven, CT, USA), and ^{13}C-labeled hydroxylated (OH)-PCBs were used internal standards; the authentic standards 4-OH-CB107 and 3-OH-CB118 for quantification were purchased from Wellington Laboratories. The standards 4-OH-CB70 and 5-OH-CB66 were provided by Dr. T. Okumura (Osaka Prefectural Government, Osaka, Japan). Microsomes containing NADPH-cytochrome P450 oxidoreductase (CPR) and the human CYP1A1, rat CYP1A1, or human CYP2D6 were purchased from BD Biosciences (San Jose, CA, USA). Microsomes containing CPR and cytochrome b_5, and the rat CYP2B1, human CYP2B6, human CYP2C9, human CYP2C19, or human CYP3A4 were also purchased from BD Biosciences. These P450 isoforms are reported to metabolize many kinds of compounds (Inui *et al.*, 2001). Microsomes containing human cytochrome b_5 and human CPR were used as controls. CB118 was dissolved in dimethyl sulfoxide (DMSO) to a final concentration of 0.77 mM.

Measurement of P450-dependent hydroxylation of CB118. The reaction solution contained 0.77 µM CB118 with a final concentration of DMSO at 0.1% (v/v), 80 nM human or rat P450 isoforms, NADPH regenerating system (0.5 mM NADPH, 5 mM glucose-6-phosphate, 1 unit glucose-6-phosphate dehydrogenase), 3.3 mM $MgCl_2$, and 100 mM potassium phosphate buffer (pH 7.4) in a total volume of 0.5 ml. The solution was allowed to react for 140 min at 37 °C with continuous shaking. Control experiments were performed using the same reaction mixtures without NADPH. Thereafter, the reaction was terminated on ice, and 10 µl 0.1 ppm ^{13}C-labeled OH-PCBs was added as an internal standard. The metabolites were extracted with four volumes of hexane and methylated as described previously (Sakiyama *et al.*, 2007). Quantification of metabolites was performed using high-resolution gas chromatography and high-resolution mass spectrometry (HRGC/HRMS: GC; 6890N [Agilent Technologies, Tokyo, Japan], MS; JMS-800D [JEOL, Tokyo, Japan]) equipped with the HT8-PCB column (Kanto Chemical, Tokyo, Japan) using SIM mode (Supplementary Table 1) under the conditions described previously (Suzuki et al., 2009). The recovery rates for metabolites were calculated using ^{13}C-2',3,4',5,5'-pentachlorobiphenyl as 61–130% and 71–130% for 3-OH-CB118 with human CYP2B6 and rat CYP2B1, respectively, and 50–140% for 4-OH-CB107 with rat CYP1A1. The limit of detection for the hydroxylated tetrachlorobiphenyls and pentachlorobiphenyls was 2.6 and 4.4 pmol (nmol P450)$^{-1}$, respectively; the limit of quantification for the hydroxylated tetrachlorobiphenyls and pentachlorobiphenyls was 8.6 and 15 pmol (nmol P450)$^{-1}$, respectively. The metabolites extracted from the reaction mixtures containing rat CYP1A1,

rat CYP2B1, or human CYP2B6 were mixed with the appropriate concentrations of the standard 4-OH-CB107 or 3-OH-CB118, and HRGC/HRMS was used to compare the retention times of the metabolites and their authentic standards.

Construction of homology models of P450 isoforms and CB118 docking models. To examine the differences in the catalytic activity of the P450 isoforms, we constructed 3D models for each P450 isoform. Rat CYP2B1 was constructed based on the X-ray crystal structure of human CYP2B6 (Gay *et al.*, 2010) using the "Mutate monomers" tool in SYBYL Biopolymer (Tripos, St. Louis, MO, USA). Docking of CB118 into the 3D models was performed using Surflex Dock in SYBYL 8.0 (Tripos) as described previously (Ruppert *et al.*, 1997). Four different amino acids constituting the substrate-binding cavities were identified in rat CYP2B1 (I104, L209, V363, and I477) and human CYP2B6 (V104, I209, L363, and V477) (Supplementary Figure 1A). Because of high amino acid identity (76%), the 3D structures of substrate-binding cavities in rat CYP2B1 and human CYP2B6 were very similar (Supplementary Figure 1B). The volume of the substrate-binding cavity of rat CYP2B1 (472 $Å^3$) was smaller than that of the human CYP2B6 (559 $Å^3$) (Supplementary Figure 1B). The 3D structure of rat CYP1A1 constructed in a previous report (Yamazaki *et al.*, 2011) was used.

Evaluation of AhR activation by CB118 and its metabolites. Animal experiments were approved by Animal Care and Use Committee of Kobe University (permission number: 26-09-08; Kobe, Japan)

and carried out according to the Animal Experimentation Regulations of Kobe University. Cytosol fractions of the livers from male Sprague-Dawley rats (6 weeks old, 200–220 g, obtained from Charles River Laboratories, Yokohama, Japan) were prepared after a quarantine period for 1 week as described previously (Ashida *et al.*, 2000).

AhR activation was measured by electrophoretic mobility shift assay (EMSA). The cytosolic fraction, containing AhR and AhR nuclear translocator, was treated with 10 ppm CB118 or its metabolites. TCDD (1 nM) was used as a positive control, and 0.1% (v/v) DMSO was used as a vehicle control. After incubation at 20 °C for 2 h, AhR activation was evaluated by EMSA (Ashida *et al.*, 2000). Briefly, 10 μg proteins from the incubated cytosol fractions were further incubated with 250 ng poly[dI-dC] (Roche Diagnostics, Basel, Switzerland) in HEDG buffer [25 mM HEPES, 1.5 mM ethylenediaminetetraacetic acid (EDTA), 1 mM dithiothreitol, and 10% (v/v) glycerol, pH 7.4] and the ^{32}P-labeled DRE probe (30 kcpm, 10 fmol) for 15 min. The mixture was then loaded onto a 4% non-stacking polyacrylamide gel in TBE buffer (25 mM Tris, 22.5 mM borate, and 0.25 mM EDTA). After electrophoresis, the AhR–DRE complex was detected by autoradiography. Densitometric analysis was carried out using ImageJ (NIH). AhR activation was evaluated as the percentage of 1 nM TCDD-induced activation.

Statistical analysis. Comparison of toxicity between CB118 and the two metabolites, 3-OH-CB118 and 4-OH-CB107, was performed by Dunnett's test (n = 4).

RESULTS

Detection of CB118 metabolites by P450 isoforms

Three NADPH-dependent metabolites of CB118 were detected in the microsomes containing rat CYP1A1 with HRGC/HRMS retention times of 26.8 min for the pentachloro metabolite and of 24 and 25 min for the tetrachloro metabolites (Figure 1C and D). In contrast, two metabolites were detected in the human CYP2B6 microsome with retention times of 28 min and 25 min for the pentachloro and tetrachloro metabolites, respectively (Figure 1G and H), and one pentachloro metabolite was detected in the rat CYP2B1 microsome with a retention time of 28 min (Figure 1I); no tetrachloro metabolites were detected in rat CYP2B1 (Figure 1J). The human CYP1A1, human CYP2C9, human CYP2C19, human CYP2D6, human CYP3A4, and control microsomal fractions did not show any NADPH-dependent peaks for the metabolites (Supplementary Figure 2).

Identification of CB118 metabolites

Because the peaks of methylated 3-OH-CB118 and 4-OH-CB107 are close to each other in the GC/MS chromatogram, we attempted to identify the metabolites by adding standards to the extract. When 4-OH-CB107 standard was added to the metabolites of rat CYP1A1, only 1 peak was detected, whereas 2 peaks were detected with the addition of the 3-OH-CB118 standard (Figure 2A and B). Hence, the pentachloro metabolite generated by the rat CYP1A1 was identified as 4-OH-CB107. For

human CYP2B6 and rat CYP2B1, the pentachloro metabolite was identified as 3-OH-CB118 (Figure 2C–F). By comparing the retention times with those of standards, the tetrachloro metabolites with rat CYP1A1 were identified as 4-OH-CB70 and 5-hydroxy-2,3',4,4'-tetrachlorobiphenyl (5-OH-CB66), and that for human CYP2B6 was identified as 5-OH-CB66 (Figure 1D and H). Proposed metabolic pathways for CB118 are shown in Figure 4.

Amounts of hydroxylated metabolites of CB118 by two P450 isoforms

The amounts of 3-OH-CB118 by human CYP2B6 and 4-OH-CB107 by rat CYP1A1 were quantified (Figure 3). Human CYP2B6 more produced 3-OH-CB118 (49 ± 8.6 pmol [nmol P450]$^{-1}$) than rat CYP1A1 did 4-OH-CB107 (6.5 ± 1.0 pmol [nmol P450]$^{-1}$) during 140-min incubation. The amounts of 5-OH-CB66 from human CYP2B6, the two tetrachloro metabolites of rat CYP1A1, and 3-OH-CB118 from rat CYP2B1 were not quantified because of their low production levels.

3D structures of P450 isoforms and its docking models with CB118

To explain the differences between the catalytic activities toward CB118, we prepared docking models of human CYP2B6 and rat CYP2B1 with CB118. Fourteen and 17 poses in the substrate-binding cavities of rat CYP2B1 (Figure 5A) and human CYP2B6 (Figure 5B), respectively, were confirmed. Differences were also observed in the poses near the heme iron. A docking model with the 3-position (C-3) of CB118 nearest to the heme iron in the substrate-binding cavity was extracted because both

P450 isoforms oxidized CB118 to 3-hydroxylated metabolites. Thereafter, we extracted the pose with the best C-3-Fe distance from the docking results and obtained models wherein the distance in human CYP2B6 was 3.6 Å (Figure 5D), and that in rat CYP2B1 was 5.8 Å (Figure 5C). As the heme Fe is the active center, the substrate-Fe distance is an important factor that needs to be considered (de Graaf *et al.*, 2005). Our models indicate that the positioning of CB118 C-3 in CYP2B6 was within catalytic distance of the Fe, whereas that in CYP2B1 was not. In contrast, rat CYP1A1 accommodated CB118 in a position accessible to the Fe; the distance between C-4 and the Fe was 5 Å.

To further understand the differences between the CB118 hydroxylation positions of the CYP2B subfamily and CYP1A1, we compared the results of the docking analysis. The rat CYP1A1 sequence has a low homology to the both CYP2Bs, which reflects the different structures of their substrate-binding cavities (Figure 6A). CYP1A1 possesses a long and narrow cavity, which is suitable for orienting the Cl-4 atom toward to the approaching Fe atom. (Figure 6B and C). The lipophilic potential of CYP1A1 is delocalized; however, CYP2Bs are localized, showing “lipophilic polarization.” Thus, the lipophilic CB118 is located higher in the lipophilic side of the cavity. Consequently, the 3-position in CB118 faces the heme Fe atom in CYP2Bs (Figure 6D and E).

EMSA

Shifted bands, which contain complexes of activated AhRs and DREs, were observed when CB118 or its metabolites 3-OH-CB118 and 4-OH-CB107 were added to cytosolic fractions of rat liver

(Supplementary Figure 3A). However, the band intensities for treatment with the two metabolites were lower than those with CB118 (Supplementary Figure 3B).

DISCUSSION

PCBs bioaccumulate in animals, including humans and wildlife, and biomagnify through the food chain. Understanding the *in vivo* metabolic fate of PCBs provides significant information toward evaluation of their toxicity. As the most predominant PCB congener in human serum is CB118 (Molto *et al.*, 2015), it is very important to elucidate the mechanisms related to its metabolic fate. In rats orally exposed to CB118, 4-OH-CB107 was identified as a major metabolite in the blood (Haraguchi *et al.*, 1998). Oxidation is the first step in metabolism of xenobiotics, and the P450 isoforms play important roles on this reaction. Our results also showed that rat CYP1A1 metabolized CB118 to 4-OH-CB107, suggesting that CYP1A1 is responsible for the production of 4-OH-CB107 from CB118 *in vivo*. Because expression of the *CYP1A1* gene is inducible by exposure to CB118 through AhR activation, it was thought that 4-OH-CB107 was produced (Hestermann *et al.*, 2000; Martin and Klaassen, 2010). Since CB118 is recognized as a mixed type inducer, the *CYP2B1* gene is also induced and 3-OH-CB118 is produced (Safe *et al.*, 1985). 4-OH-CB107 was also one of major PCB metabolites detected in human plasma samples (Quinete *et al.*, 2015). However, human CYP1A1 is probably not involved in metabolism of CB118 to 4-OH-CB107, as it did not show such activity in this study (Supplementary Figure 2C and D). Therefore, the other CYP1A subfamilies may be responsible for *in*

vivo production of 4-OH-CB107.

PCBs exhibit toxicity through at least two pathways. The first is dioxin-like toxicity through binding to AhR (Hestermann *et al.*, 2000). Our results also identified formation of the AhR-CB118 complex, to the DRE (Supplementary Figure 3). However, two metabolites, 4-OH-CB107 and 3-OH-CB118, decreased the activation of AhR. Decreased AhR activation by 4-OH-CB107 was previously shown by DR-CALUX assay (Machala *et al.*, 2004), whereas the effect of 3-OH-CB118 has not been reported to our knowledge. These results suggest that dioxin-like toxicity is decreased by the reactions of CYP1As and CYP2Bs. The second pathway of toxicity is related to hormone homeostasis. A previous report indicated that 4-OH-CB107 might affect neurodevelopment by inhibiting estrogen sulfotransferase in the human brain (Purinton and Wood, 2000). In rats, 4-OH-CB107 reduced the total T_4 levels in plasma by binding to transthyretin, resulting in defects in neurodevelopment (Meerts *et al.*, 2004b). Thus, metabolism of CB118 by CYP1A subfamilies increases toxicity through disruption of hormone homeostasis.

There are several reports on the accumulation of 3-hydroxylated metabolites from CB118 in humans (Quinete *et al.*, 2015), rats (Haraguchi *et al.*, 1998), and Baikal seals (Nomiyama *et al.*, 2014). However, the mechanisms for producing 3-OH-CB118 have not been fully clarified since it is not a major metabolite from CB118. In this study, we found that 3-OH-CB118 was produced by human CYP2B6 and rat CYP2B1 (Figure 1). CYP2B subfamilies will thus contribute to CB118 metabolism *in vivo* since CB118, a mixed type inducer, can induce gene expression for the CYP2B subfamily as

well as the CYP1A subfamily (Safe *et al.* 1985; Martin and Klaassen, 2010). Hydroxylation of CB118 by P450 isoforms has bilateral aspects such as detoxification and toxication.

Human and rat CYP2B subfamilies showed the different metabolizing activities toward CB118; human CYP2B6 showed higher 3-hydroxylation activity toward CB118 than rat CYP2B1. Two important factors differentiate their metabolizing activities towards PCBs. Four amino acids in the substrate-binding cavities were different between the human CYP2B6 and the rat CYP2B1 (Supplementary Figure 1A). Those in rat CYP2B1 were relatively larger than those in human CYP2B6, resulting in a smaller volume of the substrate-binding cavity of rat CYP2B1 (Supplementary Figure 1B). This usually results in the fewer possible poses and higher catalytic activity seen previously in metabolism of CB126 by rat CYP1A1 (Yamazaki *et al.*, 2011), where CB126 was more stably accommodated in the substrate-binding cavity of rat CYP1A1 than in that of human CYP1A1. However, rat CYP2B1 did not show higher activity than human CYP2B6. Another factor is the distance from the hydroxylation position of PCBs to the heme iron in the P450 isoforms. Our docking models showed that human CYP2B6 accommodated CB118 within 5 Å of the heme iron through stabilization by hydrophobic interaction between the 5'-position of CB118 and V104 and between the 2-position and L363. In contrast, I104 causes steric hindrance with the 5'-position of CB118 in rat CYP2B1, resulting in the lower catalytic activity of rat CYP2B1 compared to human CYP2B6. These results were supported by a previous study, which showed that the 4-position of CB126 was within 5 Å of the heme iron in rat CYP1A1, whereas no docking positions within 5 Å

were observed in human CYP1A1 (Yamazaki *et al.*, 2011). These results suggest that close proximity between PCBs and the heme iron is the more important factor for metabolizing activities.

The substrate-binding cavity of rat CYP1A1 was very different from that of the two CYP2Bs (Figure 6A). Rat CYP1A1 has a long and narrow cavity toward the heme, suggesting that 4-position of CB118 comes close to the heme iron and is subsequently hydroxylated. This was also observed for CB126 metabolism by rat CYP1A1 (Yamazaki *et al.*, 2011). In contrast, “lipophilic polarization” of the cavity was observed for CYP2Bs, which do not have long and narrow cavities like CYP1A1 (Figure 6D and E). Hydrophobic regions are advantageous for accommodation of the dichlorophenyl ring, resulting in exposure of the trichlorophenyl ring to the heme iron and subsequent hydroxylation. These results further support the importance of proximity between the 3-posittion of CB118 and the heme iron, owing to “lipophilic polarization” of the cavity, in determining the hydroxylation activity. Furthermore, this pose is determined and maintained by interaction with peripheral amino acids.

The present study clearly showed the structural basis of hydroxylation positions of CB118 by CYP2Bs and CYP1A1 through docking models. Furthermore, although decreased dioxin-like toxicity of CB118 through metabolism by CYP2Bs was demonstrated, toxicity from increased levels of 4-OH-CB107 can occur through disruption of hormone regulation (Purinton and Wood, 2000; Meerts *et al.*, 2004b). These P450 isoforms play an important role in determining the toxicity of CB118. This study will contribute to understanding the metabolic fate and toxicity of CB118 *in vivo*, and this experimental strategy can be applied to evaluate the *in vivo* toxicity of other PCB congeners.

SUPPLEMENTARY DATA DESCRIPTION

Supplementary Figure 1. Comparison of the amino acids sequence of rat CYP2B1 and human CYP2B6 (A) and their 3D structures (B).

Supplementary Figure 2. HRGC/HRMS analyses of pentachloro (A, C, E, G, I, and K) and tetrachloro (B, D, F, H, J, and L) metabolites of mammalian P450 isoforms.

Supplementary Figure 3. EMSA for CB118 and its metabolites.

Supplementary Table 1. Selected ion of derivatized hydroxylated PCBs

FUNDING INFORMATION

This work was supported by a Grant-in-Aid for Challenging Exploratory Research [grant number 25550064] from the Japan Society for the Promotion of Science.

REFERENCES

Ashida, H., Fukuda, I., Yamashita, T., and Kanazawa, K. (2000). Flavones and flavonols at dietary levels inhibit a transformation of aryl hydrocarbon receptor induced by dioxin. *FEBS Lett.* **476**(3), 213-217.

de Graaf, C., Pospisil, P., Pos, W., Folkers, G., and Vermeulen, N. P. (2005). Binding mode prediction of cytochrome p450 and thymidine kinase protein-ligand complexes by consideration of water and rescoring in automated docking. *J. Med. Chem.* **48**(7), 2308-2318.

Gay, S. C., Shah, M. B., Talakad, J. C., Maekawa, K., Roberts, A. G., Wilderman, P. R., Sun, L., Yang, J. Y., Huelga, S. C., Hong, W. X., Zhang, Q., Stout, C. D., and Halpert, J. R. (2010). Crystal structure of a cytochrome P450 2B6 genetic variant in complex with the inhibitor 4-(4-chlorophenyl)imidazole at 2.0-A resolution. *Mol. Pharmacol.* **77**(4), 529-538.

Haraguchi, K., Kato, Y., Kimura, R., and Masuda, Y. (1998). Hydroxylation and methylthiolation of mono-*ortho*-substituted polychlorinated biphenyls in rats: identification of metabolites with tissue affinity. *Chem. Res. Toxicol.* **11**(12), 1508-1515.

Hestermann, E. V., Stegeman, J. J., and Hahn, M. E. (2000). Relative contributions of affinity and intrinsic efficacy to aryl hydrocarbon receptor ligand potency. *Toxicol. Appl. Pharmacol.* **168**(2), 160-172.

Hirai, T., Fujimine, Y., Watanabe, S., and Nakano, T. (2005). Congener-specific analysis of polychlorinated biphenyl in human blood from Japanese. *Environ. Geochem. Health* **27**(1), 65-73.

Imaeda, D., Nomiyama, K., Kunisue, T., Iwata, H., Tsydenova, O., Amano, M., Petrov, E. A., Batoev, V. B., and Tanabe, S. (2014). Blood levels of polychlorinated biphenyls and their hydroxylated metabolites in Baikal seals (*Pusa sibirica*): emphasis on interspecies comparison, gender difference and association with blood thyroid hormone levels. *Chemosphere* **114**, 1-8.

Inui, H., Shiota, N., Motoi, Y., Ido, Y., Inoue, T., Kodama, T., Ohkawa, Y., and Ohkawa, H. (2001). Metabolism of herbicides and other chemicals in human cytochrome P450 species and in transgenic potato plants co-expressing human CYP1A1, CYP2B6 and CYP2C19, *J. Pestic. Sci.* **26**, 28-40

Inui, H., Itoh, T., Yamamoto, K., Ikushiro, S., and Sakaki, T. (2014). Mammalian cytochrome P450-dependent metabolism of polychlorinated dibenzo-*p*-dioxins and coplanar polychlorinated biphenyls. *Int. J. Mol. Sci.* **15**(8), 14044-14057.

Kania-Korwel, I., Duffel, M. W., and Lehmler, H. J. (2011). Gas chromatographic analysis with chiral cyclodextrin phases reveals the enantioselective formation of hydroxylated polychlorinated biphenyls by rat liver microsomes. *Environ. Sci. Technol.* **45**(22), 9590-9596.

Londoño, M., Shimokawa, N., Miyazaki, W., Iwasaki, T., and Koibuchi, N. (2009). Hydroxylated PCB induces Ca2+ oscillations and alterations of membrane potential in cultured cortical cells. *J. Appl. Toxicol.* **30**, 334-342

Machala, M., Bláha, L., Lehmler, H.-J., Plíšková, M., Májková, Z., Kapplová, P., Sovadinová, I., Vondráček, J., Malmberg, T., and Robertson, L. W. (2004). Toxicity of hydroxylated and quinoid PCB Metabolites: Inhibition of gap junctional intercellular communication and activation of aryl hydrocarbon and estrogen receptors in hepatic and mammary cells. *Chem. Res. Toxicol.* **17**, 340-347.

Martin, L., and Klaassen, C. D. (2010). Differential effects of polychlorinated biphenyl congeners on serum thyroid hormone levels in rats. *Toxicol. Sci.* **117**(1), 36-44.

McGraw Sr., J. E. and Waller, D. P. (2006). Specific human CYP 450 isoform metabolism of a pentachlorobiphenyl (PCB-IUPAC# 101). *Biochem. Biophys. Res. Commun.* **344**, 129-133

Meerts, I. A., Hoving, S., van den Berg, J. H., Weijers, B. M., Swarts, H. J., van der Beek, E. M., Bergman, A., Koeman, J. H., and Brouwer, A. (2004a). Effects of in utero exposure to 4-hydroxy-2,3,3',4',5-pentachlorobiphenyl (4-OH-CB107) on developmental landmarks, steroid hormone levels, and female estrous cyclicity in rats. *Toxicol. Sci.* **82**(1), 259-267.

Meerts, I. A., Lilienthal, H., Hoving, S., van den Berg, J. H., Weijers, B. M., Bergman, A., Koeman, J. H., and Brouwer, A. (2004b). Developmental exposure to 4-hydroxy-2,3,3',4',5-pentachlorobiphenyl (4-OH-CB107): long-term effects on brain development, behavior, and brain stem auditory evoked potentials in rats. *Toxicol. Sci.* **82**(1), 207-218.

Mimura, J., and Fujii-Kuriyama, Y. (2003). Functional role of AhR in the expression of toxic effects by TCDD. *Biochim. Biophys. Acta* **1619**(3), 263-268.

Molto, J., Paul, R., Ortuno, N., Medrano, M. L., Aizpurua, J., and Gomez-Torres, M. J. (2015). Levels of dioxin-like PCBs in low-volume serum samples of male patients attending fertility clinics. *Environ. Sci. Pollut. Res. Int.* doi: 10.1007/s11356-015-5571-7.

Nomiyama, K., Hirakawa, S., Eguchi, A., Kanbara, C., Imaeda, D., Yoo, J., Kunisue, T., Kim, E. Y., Iwata, H., and Tanabe, S. (2014). Toxicological assessment of polychlorinated biphenyls and their metabolites in the liver of Baikal seal (*Pusa sibirica*). *Environ. Sci. Technol.* **48**(22), 13530-13539.

Nunes, M., Marchand, P., Vernisseau, A., Le Bizec, B., Ramos, F., and Pardal, M. A. (2011). PCDD/Fs and dioxin-like PCBs in sediment and biota from the Mondego estuary (Portugal). *Chemosphere* **83**(10), 1345-1352.

Purinton, S. C., and Wood, C. E. (2000). Ovine fetal estrogen sulfotransferase in brain regions important for hypothalamus-pituitary-adrenal axis control. *Neuroendocrinology* **71**(4), 237-242.

Quinete, N., Kraus, T., Belov, V. N., Aretz, C., Esser, A., and Schettgen, T. (2015). Fast determination of hydroxylated polychlorinated biphenyls in human plasma by online solid phase extraction coupled to liquid chromatography-tandem mass spectrometry. *Anal. Chim. Acta* **888**, 94-102.

Ruppert, J., Welch, W., and Jain, A. N. (1997). Automatic identification and representation of protein binding sites for molecular docking. *Protein Sci.* **6**(3), 524-533.

Safe, S., Bandiera, S., Sawyer, T., Robertson, L., Safe, L., Parkinson, A., Thomas, P. E., Ryan, D. E., Reik, L. M., Levin, W., Denomme, M. A., and Fujita, T. (1985). PCBs: Structure-function relationships and mechanism of action. *Environ. Health Perspect.* **60**, 47-56.

Sakiyama, T., Yamamoto, A., Kakutani, N., Fukuyama, J., and Okumura, T. (2007). Hydroxylated polychlorinated biphenyls (OH-PCBs) in the aquatic environment: levels and congener profiles in sediments from Osaka, Japan. *Organohal. Comp.* **69**, 1380-1383.

Suzuki, M., Takemine, S., Tsurukawa, M., Matsumura, C., Nakano, T., and Imaishi, H. (2009). Investigation of hydroxylated polychlorinated biphenyls (OH-PCBs) in the air and the sediments around the paper recycling plant. *Organohal. Comp.* **71**, 1881-1885.

Van den Berg, M., Birnbaum, L. S., Denison, M., De Vito, M., Farland, W., Feeley, M., Fiedler, H., Hakansson, H., Hanberg, A., Haws, L., Rose, M., Safe, S., Schrenk, D., Tohyama, C., Tritscher, A., Tuomisto, J., Tysklind, M., Walker, N., and Peterson, R. E. (2006). The 2005 World Health Organization reevaluation of human and Mammalian toxic equivalency factors for dioxins and dioxin-like compounds. *Toxicol. Sci.* **93**(2), 223-241.

Yamazaki, K., Suzuki, M., Itoh, T., Yamamoto, K., Kanemitsu, M., Matsumura, C., Nakano, T., Sakaki, T., Fukami, Y., Imaishi, H., and Inui, H. (2011). Structural basis of species differences between human and experimental animal CYP1A1s in metabolism of 3,3',4,4',5-pentachlorobiphenyl. *J. Biochem.* **149**(4), 487-494.

FIGURE LEGENDS

Figure 1. HRGC/HRMS analyses of pentachloro (A, C, E, G, and I) and tetrachloro (B, D, F, H, and J) metabolites of CB118 by rat CYP1A1 (C and D), human CYP2B6 (G and H), and rat CYP2B1 (I and J).

The authentic standards are shown in A and E for MeO-pentachlorobiphenyls and in B and F for MeO-tetrachlorobiphenyls. Peak 1, 4-MeO-CB107; peak 2, 4-MeO-CB70; peak 3, 5-MeO-CB66;

peak 4, 3-MeO-CB118. The reaction solution contained 0.77 μM CB118, 80 nM human or rat P450 isoforms, NADPH regenerating system, 3.3 mM $MgCl_2$, and 100 mM potassium phosphate buffer (pH 7.4) in a total volume of 0.5 ml. The solution was allowed to react for 140 min at 37 °C with continuous shaking. NADPH-dependent peaks show metabolites generated by P450 reactions. Three, two, and one metabolites were detected in rat CYP1A1, human CYP2B6, and rat CYP2B1, respectively.

Figure 2. Comparison of retention times for metabolites and authentic standards.

Peak 1, 4-MeO-CB107; peak 4, 3-MeO-CB118. (A and B) Addition of the standards 3-OH-CB118 (A) and 4-OH-CB107 (B) to metabolites from rat CYP1A1. (C and D) Addition of the standards 3-OH-CB118 (C) and 4-OH-CB107 (D) to metabolites from human CYP2B6. (E and F) Addition of the standards 3-OH-CB118 (E) and 4-OH-CB107 (F) to metabolites from rat CYP2B1. Arrows indicate the peaks of metabolites. Rat CYP1A1 metabolized CB118 to 4-OH-CB107, whereas human CYP2B6 and rat CYP2B1 metabolized CB118 to 3-OH-CB118.

Figure 3. The amount of hydroxylated metabolites of CB118 by human CYP2B6 and by rat CYP1A1.

The amounts of 3-OH-CB118 from human CYP2B6 and 4-OH-CB107 from rat CYP1A1 were shown. The amounts of hydroxylated metabolites were calculated by subtraction of those without NADPH from those with NADPH in the reaction mixture. Results are expressed as the mean ± SD (n = 4,

human CYP2B6; *n* = 5, rat CYP1A1). Human CYP2B6 more produced 3-OH-CB118 than rat CYP1A1 did 4-OH-CB107.

Figure 4. Proposed metabolic pathways for CB118 by human CYP2B6, rat CYP2B1, and rat CYP1A1.

The arrow thickness indicates the level of hydroxylation activity.

Figure 5. Conformations of CB118 in the substrate-binding cavities of rat CYP2B1 and human CYP2B6.

Rat CYP2B1 was constructed based on the X-ray crystal structure of human CYP2B6 (Gay *et al.*, 2010) using the "Mutate monomers" tool in SYBYL Biopolymer. Docking of CB118 into the 3D models was performed using Surflex Dock in SYBYL 8.0 as described previously (Ruppert *et al.*, 1997). Substrate-binding cavities are shown in mesh. In each cavity, the accommodated CB118 is shown as sticks. The size of the substrate-binding cavity in rat CYP2B1 was 472 $Å^3$. The 14 poses of CB118 identified in the docking study are represented (A). In contrast, the size of a substrate-binding cavity in human CYP2B6 was 559 $Å^3$. The 17 poses of CB118 identified in the docking study are represented (B). The distance between the C-3 position of CB118 and the heme iron was 5.8 Å for rat CYP2B1 (C) and 3.6 Å for human CYP2B6 (D). Close proximity between the hydroxylation position of CB118 and the heme iron was important for metabolic activity.

Figure 6. Structure and lipophilic potential of the substrate binding cavities of human CYP2B6, rat CYP2B1, and rat CYP1A1.

(A) Structural differences in the substrate-binding cavities of human CYP2B6 (red) and rat CYP1A1 (yellow). (B–E) The lipophilic potential of the substrate binding cavities of rat CYP1A1 (B and C), human CYP2B6 (D), and rat CYP2B1 (E) is mapped in color as lipophilicity. The shape and lipophilic potential of the substrate-binding cavities influenced the hydroxylation position of CB118.

Supplementary Table 1 Selected ion of derivatized hydroxylated PCBs

Homologue	Derivatized homologue	Selected fragment (*m*/*z*)
OH-TeCBs[1]	CH_3O-TeCBs	321.9301 $[M+2]^+$
		319.9329 $[M]^+$
		278.9116 $[M+2\text{-}COCH_3]^+$
		269.9406 $[M\text{-}ClCH_3]^+$
OH-PeCBs[2]	CH_3O-PeCBs	355.8911 $[M+2]^+$
		357.8882 $[M+4]^+$
		312.8727 $[M+2\text{-}COCH_3]^+$
		305.8987 $[M+2\text{-}ClCH_3]^+$
OH-[$^{13}C_{12}$]-TeCB	CH_3O-[$^{13}C_{12}$]-TeCB	333.9702 $[M+2]^+$
OH-[$^{13}C_{12}$]-PeCB	CH_3O-[$^{13}C_{12}$]-PeCB	365.9342 $[M]^+$
[$^{13}C_{12}$]-2,3',4',5-TeCB		303.9597 $[M+2]^+$

[1]Tetrachlorobiphenyl; [2]Pentachlorobiphenyl

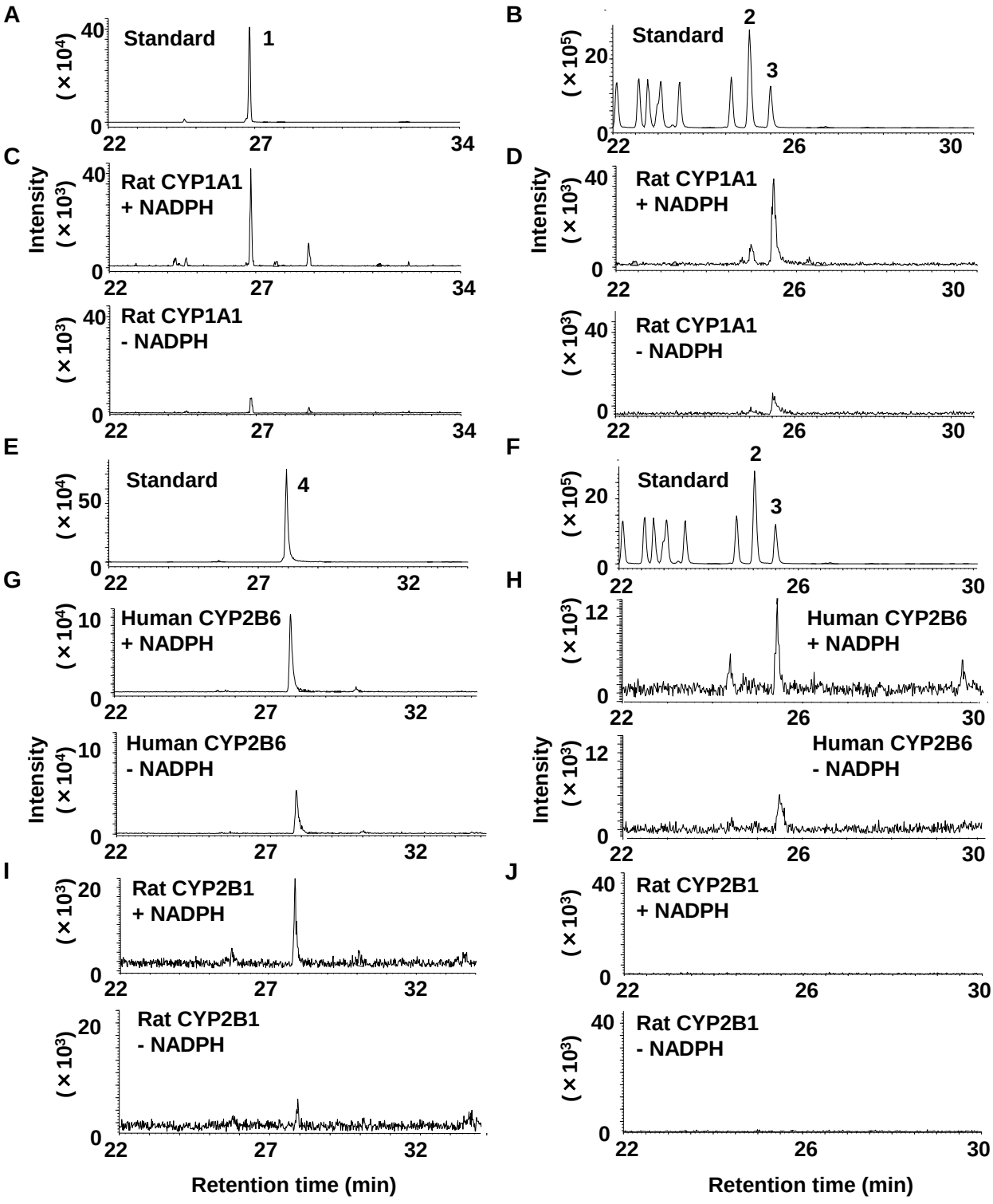

A
Standard
1
B
Standard
2
3
C
Rat CYP1A1
+ NADPH
Rat CYP1A1
- NADPH
D
Rat CYP1A1
+ NADPH
Rat CYP1A1
- NADPH
E
Standard
4
F
Standard
2
3
G
Human CYP2B6
+ NADPH
Human CYP2B6
- NADPH
H
Human CYP2B6
+ NADPH
Human CYP2B6
- NADPH
I
Rat CYP2B1
+ NADPH
Rat CYP2B1
- NADPH
J
Rat CYP2B1
+ NADPH
Rat CYP2B1
- NADPH
Intensity
Retention time (min)
Retention time (min)

Figure 1.

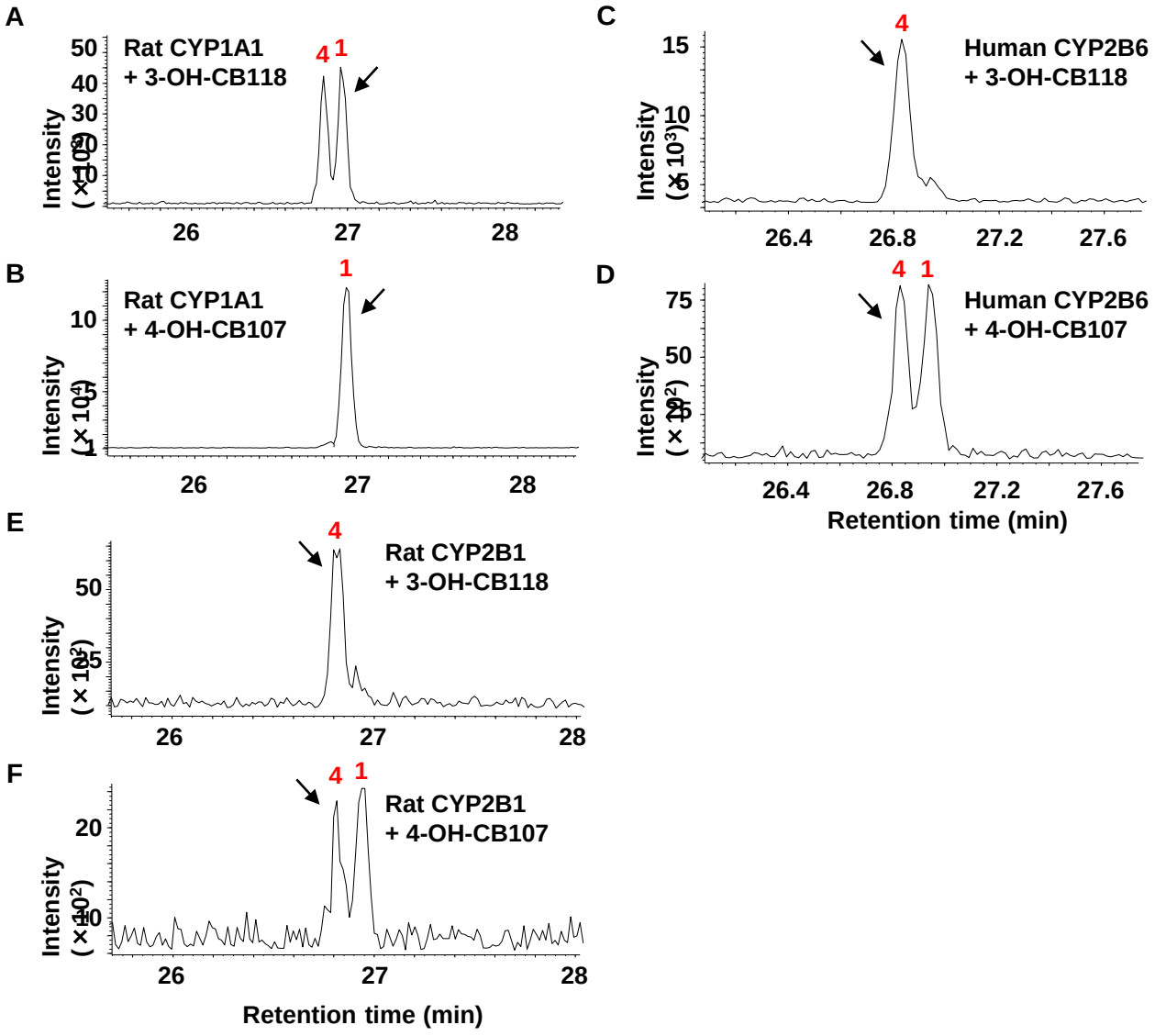

A
Rat CYP1A1
+ 3-OH-CB118
4
1
Intensity
B
Rat CYP1A1
+ 4-OH-CB107
1
C
Human CYP2B6
+ 3-OH-CB118
4
D
Human CYP2B6
+ 4-OH-CB107
4
1
E
Rat CYP2B1
+ 3-OH-CB118
4
F
Rat CYP2B1
+ 4-OH-CB107
4
1
26
27
28
26.4
26.8
27.2
27.6
Retention time (min)

Figure 2.

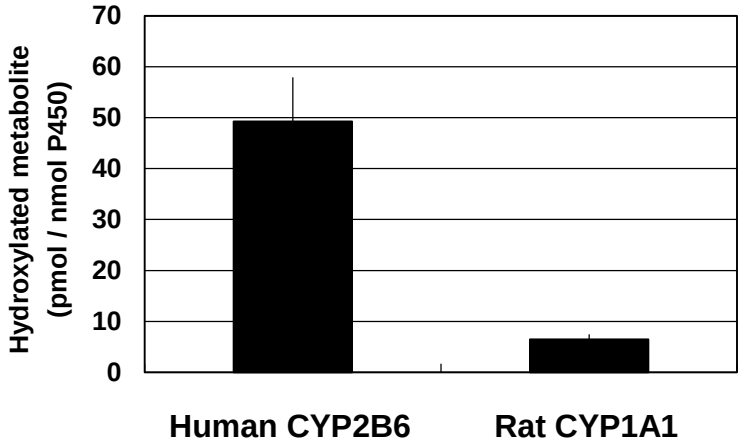

Hydroxylated metabolite
(pmol / nmol P450)
70
60
50
40
30
20
10
0
Human CYP2B6
Rat CYP1A1

Figure 3.

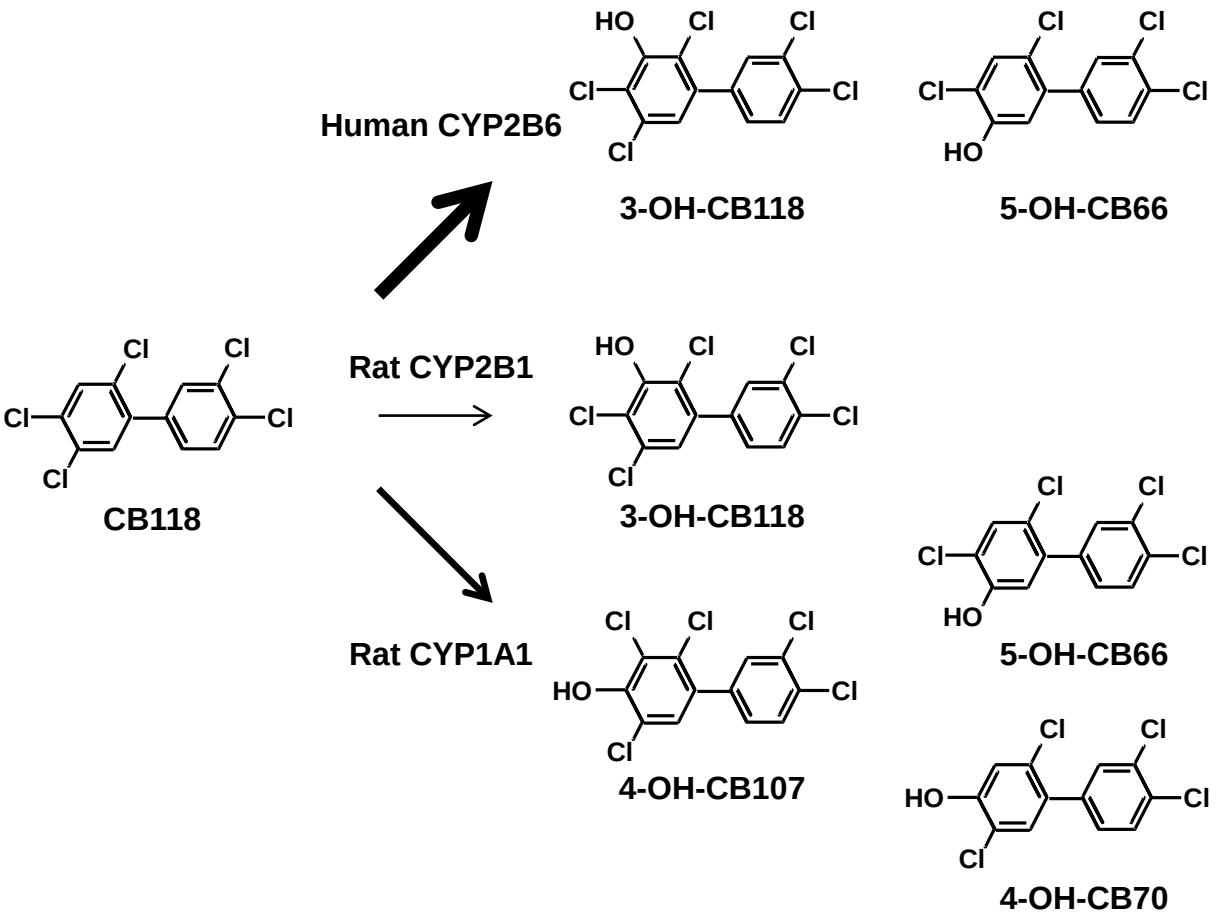

Human CYP2B6
Rat CYP2B1
Rat CYP1A1
CB118
3-OH-CB118
5-OH-CB66
3-OH-CB118
5-OH-CB66
4-OH-CB107
4-OH-CB70

Figure 4.

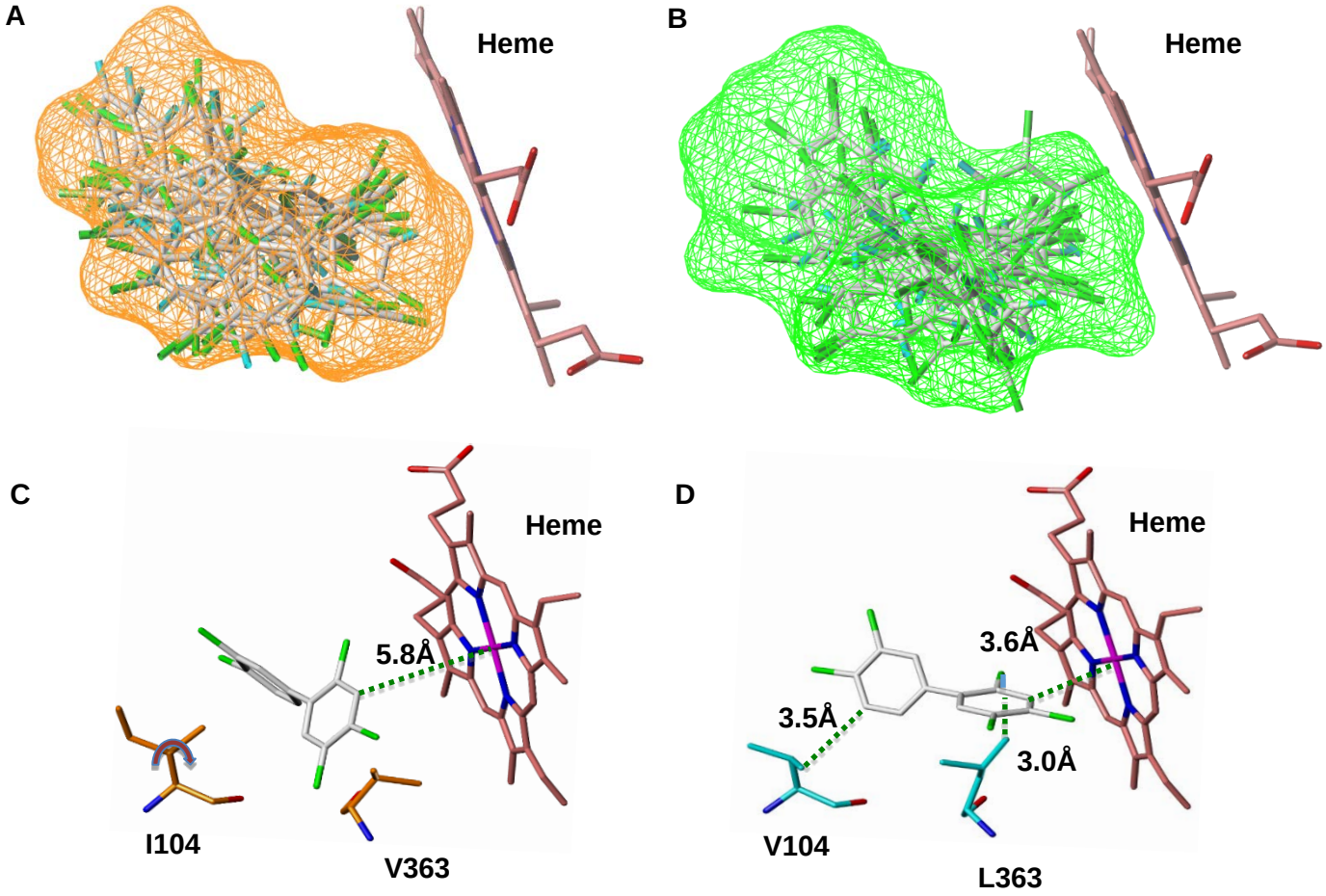


Figure 5.

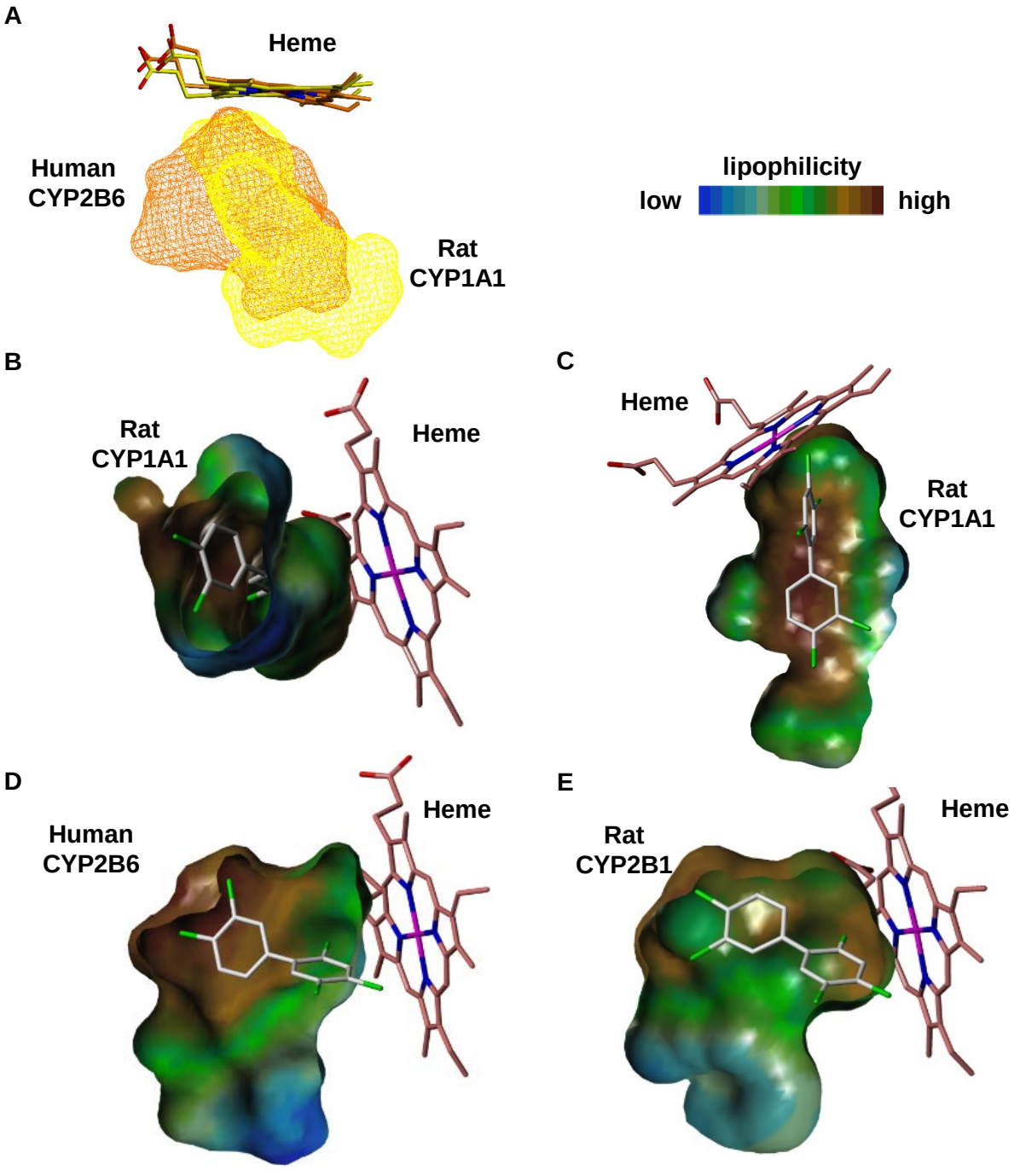

A
Heme
Human
CYP2B6
Rat
CYP1A1
lipophilicity
low
high
B
Rat
CYP1A1
Heme
C
Heme
Rat
CYP1A1
D
Human
CYP2B6
Heme
E
Rat
CYP2B1
Heme

Figure 6.

A

```
  1 MEPSILLLLALLVGFLLLLVRGHPKSRGNFPPGPRPLPLLGNLLQLDRGGLLNSFMQLREKYGDVFTVHLGPRPVVMLCGTDTIKEALVGQAEDFSGRGT 101
  1 MELSVLLFLALLTGLLLLLVQRHPNTHDRLPPGPRPLPLLGNLLQMDRRGLLKSFLRFREKYGDVFTVHLGPRPVVMLCGVEAIREALVDKAEAFSGRGK 101
    ** * ** **** * *****  **      ********** ** *** **   ********************   * ****  ** *****

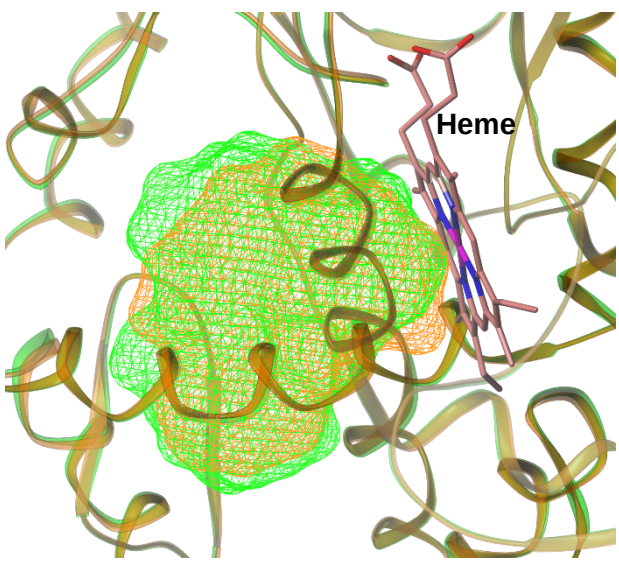
101 IAVIEPIFKEYGVIFANGERWKALRRFSLATMRDFGMGKRSVEERIQEEAQCLVEELRKSQGAPLDPTFLFQCITANIICSIVFGERFDYTDRQFLRLLE 201
101 IAMVDPFFRGYGVIFANGNRWKVLRRFSVTTMRDFGMGKRSVEERIQEEAQCLIEELRKSKGALMDPTFLFQSITANIICSIVFGKRFHYQDQEFLKMLN 201
    **   * *  ******** *** *****  ********************** ****** **  ******* ********** ** * *  **  *

201 LFYRTFSLLSSFSSQVFEFFSGFLKYFPGAHRQISKNLQEILDYIGHIVEKHRATLDPSAPRDFIDTYLLRMEKEKSNHHTVFHHENLMISLLSLFFAGT 301
201 LFYQTFSLISSVFGQLFELFSGFLKYFPGAHRQVYKNLQEINAYIGHSVEKHRETLDPSAPKDLIDTYLLHMEKEKSNAHSEFSHQNLNLNTLSLFFAGT 301
    *** **** **   * ** **********  ******  **** ***** ******* * ****** ******* *  * * * **    ********

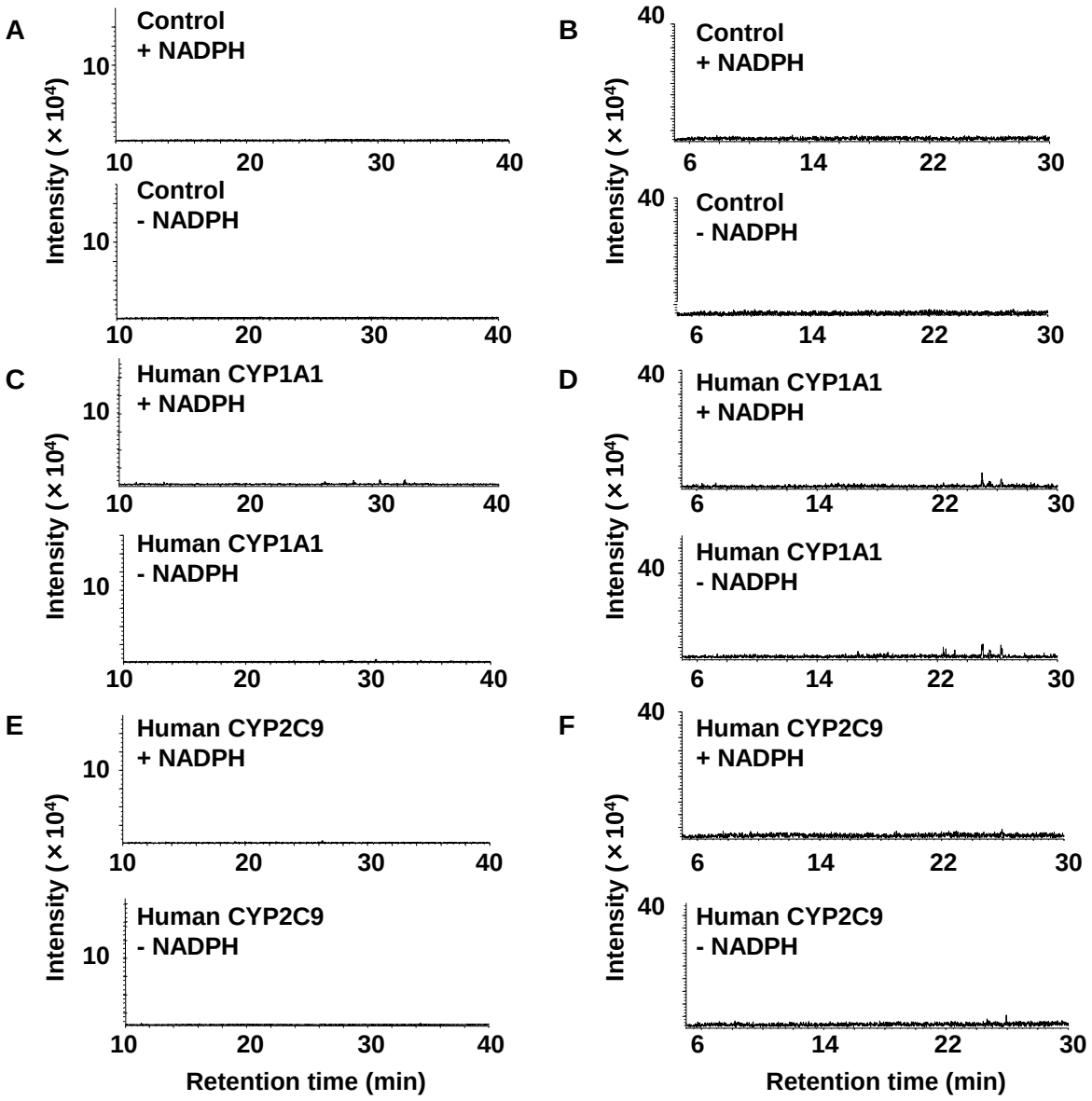
301 ETSSTTLRYGFLLMLKYPHVAEKVQKEIDQVIGSHRLPTLDDRSKMPYTDAVIHEIQRFSDLVPIGVPHRVTKDTMFRGYLLPKNTEVYPILSSALHDPQ 401
301 ETTSTTLRYGFLLMLKYPHVAERVYREIEQVIGPHRPPELHDRAKMPYTEAVIYEIQRFSDLLPMGVPHIVTQHTSFRGYIIPKDTEVFLILSTALHDPH 401
    ** ******************** *  ** **** ** * * ** ***** *** ******** * **** **  * ****  ** ***  *** *****

401 YFDHPDSFNPEHFLDANGALKKSEAFMPFSTGKRICLGEGIARNELFLFFTTILQNFSVSSHLAPKDIDLTPKESGIGKIPPTYQICFSAR 491
401 YFEKPDAFNPDHFLDANGALKKTEAFIPFSLGKRICLGEGIARAELFLFFTTILQNFSMASPVAPEDIDLTPQECGVGKIPPTYQIRFLPR 491
    **  ** *** ********** *** *** ********** **********  *  ** ****** * * ********* *  *
```

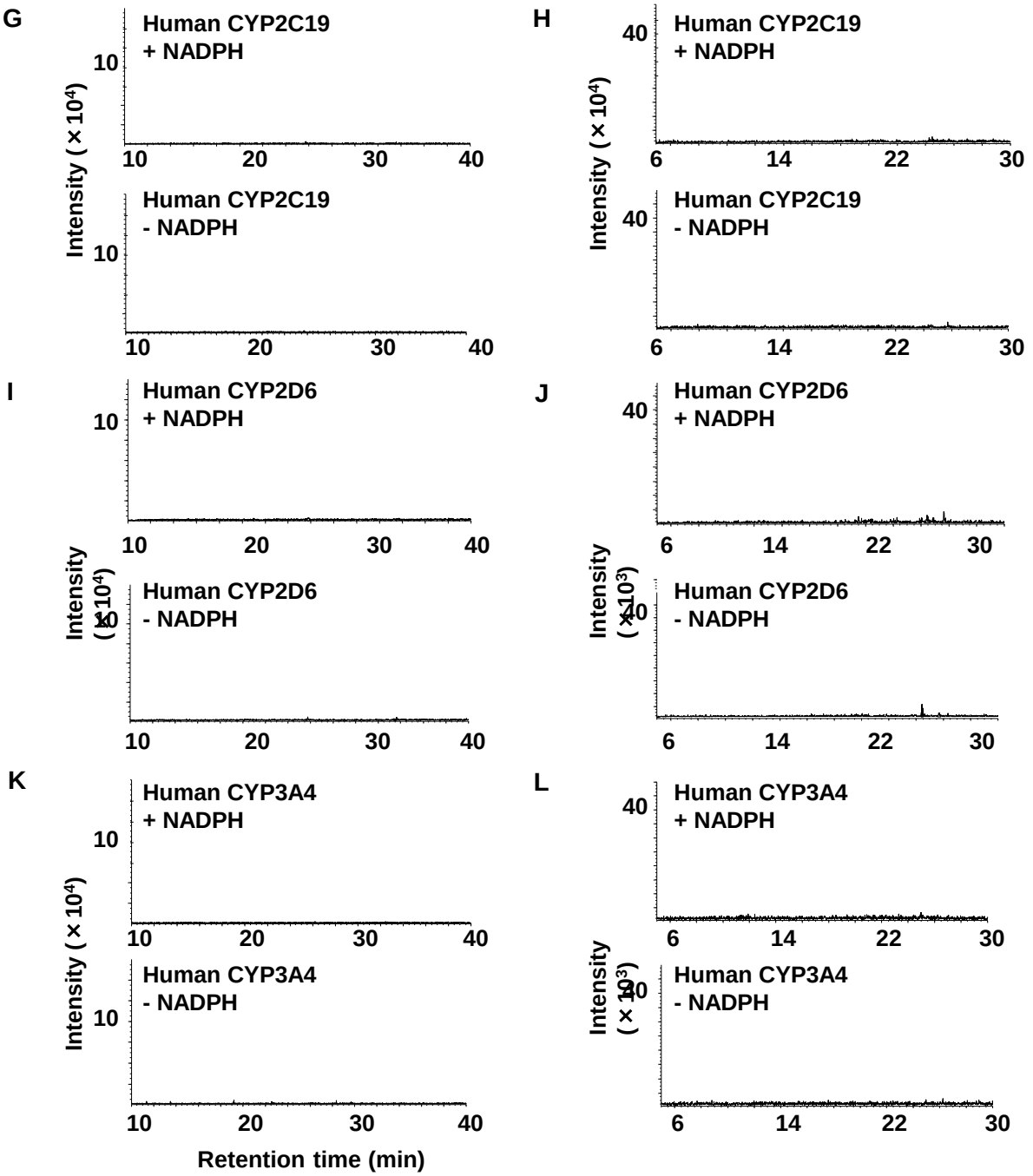
B



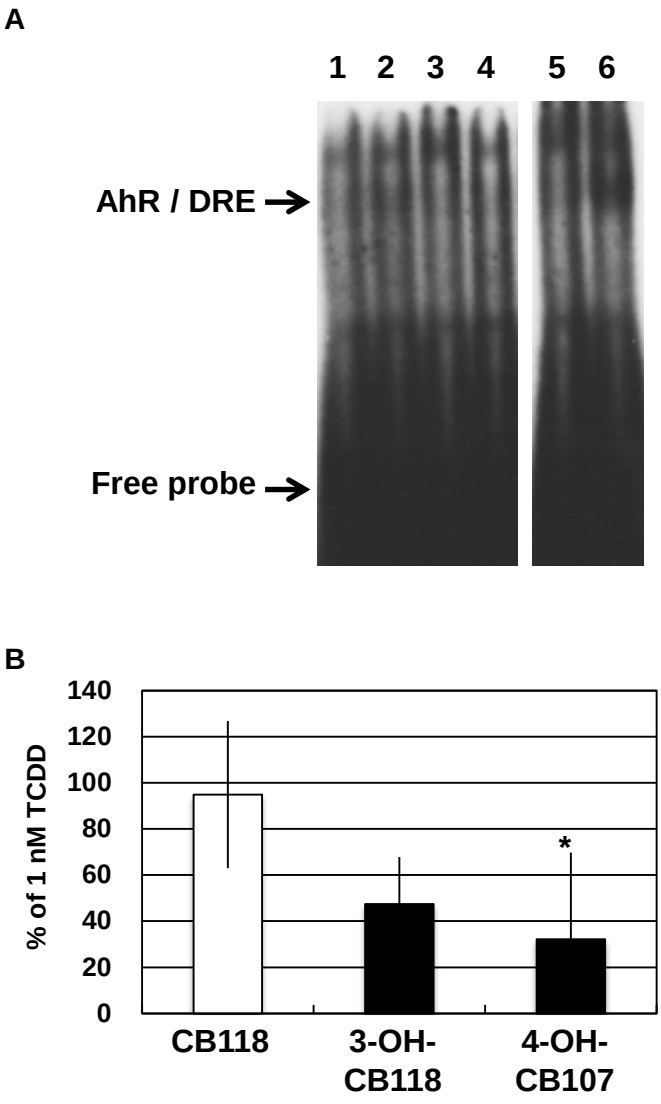
Supplementary Figure 1. Comparison of the amino acids sequence of rat CYP2B1 and human CYP2B6 (A) and their 3D structures (B).
Arrows show the different amino acids constituting the substrate-binding pocket. Asterisks show the identical amino acids between rat CYP2B1 (red) and human CYP2B6 (green).



Supplementary Figure 2. HRGC/HRMS analyses of pentachloro (A, C, E, G, I, and K) and tetrachloro (B, D, F, H, J, and L) metabolites of mammalian P450 isoforms.
Control microsomes containing human cytochrome b_5 and human NADPH-P450 oxidoreductase (A and B), microsomes containing human CYP1A1 (C and D), human CYP2C9 (E and F), human CYP2C19 (G and H), human CYP2D6 (I and J), and human CYP3A4 (K and L).



Supplementary Figure 2. continued



Supplementary Figure 3. EMSA for CB118 and its metabolites.
The cytosolic fraction, containing AhR and AhR nuclear translocator, was treated with 10 ppm CB118 or its metabolites. TCDD was used as a positive control, and 0.1% (v/v) DMSO was used as a vehicle control. After incubation at 20 ° C for 2 h, 10 mg proteins from the incubated cytosol fractions were further incubated with 250 ng poly[dI-dC] and the ^{32}P-labeled DRE probe for 15 min. The mixture was then loaded onto a 4% non-stacking polyacrylamide gel. After electrophoresis, the AhR–DRE complex was detected by autoradiography. Densitometric analysis was carried out using ImageJ. (A) Lane 1, 0.1% DMSO; lane 2, 10 ppm CB118; lane 3, 10ppm 3-OH-CB118; lane 4, 10 ppm 4-OH-CB107; lane 5, 0.1% DMSO; lane 6, 1 nM TCDD. (B) Activation of AhR is expressed as % of 1 nM TCDD. Results are expressed as the mean ± SD (n = 4). * P < 0.05 by Dunnett's test.